40

JAERI-Research
97-056

NOV 12 1997

EVALUATION OF NEUTRON NUCLEAR DATA FOR ^{247}CM AND ^{247}BK

JAERI-Research-97-056

Fermilab Library
0 1160 0059278 4

August 1997

Tsuneo NAKAGAWA※ and LIU Tong*

日本原子力研究所
Japan Atomic Energy Research Institute

本レポートは，日本原子力研究所が不定期に公刊している研究報告書です。
入手の問合わせは，日本原子力研究所研究情報部研究情報課（〒319-11 茨城県那珂郡東海村）あて，お申し越しください。なお，このほかに財団法人原子力弘済会資料センター（〒319-11 茨城県那珂郡東海村日本原子力研究所内）で複写による実費頒布をおこなっております。

This report is issued irregularly.
Inquiries about availability of the reports should be addressed to Research Information Division, Department of Intellectual Resources, Japan Atomic Energy Research Institute, Tokai-mura, Naka-gun, Ibaraki-ken, 319-11, Japan.

© Japan Atomic Energy Research Institute, 1997

編集兼発行　日本原子力研究所
印　　刷　いばらき印刷㈱

JAERI-Research 97-056

Evaluation of Neutron Nuclear Data for ^{247}Cm and ^{247}Bk

Tsuneo NAKAGAWA※ and LIU Tong*

Department of Reactor Engineering
Tokai Research Establishment
Japan Atomic Energy Research Institute
Tokai-mura, Naka-gun, Ibaraki-ken

(Received July 23, 1997)

The neutron nuclear data for ^{247}Cm and ^{247}Bk were evaluated for JENDL Actinide File. As for ^{247}Cm, the drawbacks in the previous evaluation have been removed. For ^{247}Bk the present work provided the first evaluation in the world. The evaluation for both nuclides was made in the neutron energy range from 10^{-5} eV to 20 MeV. Finally recommended data are the total, elastic scattering, inelastic scattering, fission, capture, (n,2n) and (n,3n) reaction cross sections, resonance parameters, angular distributions and energy spectra of emitted neutrons and number of neutrons per fission.

Keywords: Neutron, Evaluation, Data, Curium-247, Berkelium-247

※On loan to Nuclear Power Engineering Corporation

*Chinese Nuclear Data Center, China Institute of Atomic Energy

JAERI-Research 97-056

^{247}Cmと^{247}Bkの中性子核データの評価

日本原子力研究所東海研究所原子炉工学部
中川　康雄※・Liu Tong*

（1997年7月23日受理）

ＪＥＮＤＬ Actinide Fileに格納するために、^{247}Cmと^{247}Bkの中性子核データの評価を行った。^{247}Cmに関しては、前回の評価結果に見られた問題点を改良した。今回の^{247}Bkの評価は世界で始めてのものである。両方の核種に対して、中性子エネルギー10^{-5}eVから20MeVの範囲で評価を行い、全断面積、弾性・非弾性散乱断面積、核分裂断面積、捕獲断面積、（ｎ，２ｎ）と（ｎ，３ｎ）反応断面積、共鳴パラメータ、放出中性子の角度分布とエネルギースペクトル、および核分裂あたりの放出中性子数の推奨値を求めた。

東海研究所：〒319－11　茨城県那珂郡東海村白方白根２－４
※ 出向中：㈶原子力発電技術機構
＊ 中国原子能科学研究院中国核データセンター

Contents

1. Introduction 1
2. Evaluation of ^{247}Cm Nuclear Data 2
2.1 Review of Previous Evaluation 2
2.2 Reevaluation 4
2.2.1 Resonance Parameters 4
2.2.2 Inelastic Scattering Cross Sections 5
2.2.3 (n,2n),(n,3n) and (n,4n) Reaction Cross Sections 7
2.2.4 Fission Cross Section 7
2.2.5 Other Cross Sections 7
2.2.6 Other Data 8
2.3 Conclusion 9
3. Evaluation of ^{247}Bk Nuclear Data 10
3.1 Thermal Cross Sections 10
3.2 Resonance Parameters 11
3.3 Cross Sections above Resonance Region 11
3.4 Angular Distributions of Emitted Neutrons 12
3.5 Energy Distributions of Emitted Neutrons 12
3.6 Number of Neutrons per Fission 13
3.7 Conclusion 13
Acknowledgment 14
References 14

目　　次

1. はじめに …… 1
2. ^{247}Cmの核データ評価 …… 2
2.1 前回の評価のレビュー …… 2
2.2 再評価 …… 4
2.2.1 共鳴パラメータ …… 4
2.2.2 非弾性散乱断面積 …… 5
2.2.3 (n, 2n)、(n, 3n) および (n, 4n) 反応断面積 …… 7
2.2.4 核分裂断面積 …… 7
2.2.5 その他の断面積 …… 7
2.2.6 その他のデータ …… 8
2.3 結論 …… 9
3. ^{247}Bkの核データの評価 …… 10
3.1 熱中性子断面積 …… 10
3.2 共鳴パラメータ …… 11
3.3 共鳴領域より上の断面積 …… 11
3.4 放出中性子の角度分布 …… 12
3.5 放出中性子のエネルギー分布 …… 12
3.6 核分裂あたりの放出中性子数 …… 13
3.7 結論 …… 13
謝　辞 …… 14
参考文献 …… 14

1. Introduction

Research on transmutation of high level radioactive nuclides in spent fuel has become important. The nuclear data of minor actinide nuclides are needed in this field as basic data for the research. In order to provide the data of minor actinide nuclides that are not important in ordinary fission reactors, JENDL Actinide File[1)] is being made at the Nuclear Data Center of Japan Atomic Energy Research Institute, and it will include evaluated nuclear data for minor actinides with a half-life longer than 1 day including such major nuclides as ^{235}U, ^{238}U, ^{239}Pu.

In the present work, evaluation of nuclear data for ^{247}Cm and ^{247}Bk was made so as to provide the data for JENDL Actinide File. The data of ^{247}Cm[2)] are already given in JENDL-3.2[3)] which is the latest version of Japanese Evaluated Nuclear Data Library. However, its fission cross section is inconsistent with recent experimental data[4)]. Some problems have been indicated[5)]: cross-section data of the inelastic scattering, (n,2n) and (n,3n) reactions in the high energy region. In the present evaluation, these data were improved. On the other hand, no evaluated data exist for ^{247}Bk while it has a half-life of 1380 years. The reason is that the nuclide of ^{247}Bk is not easily produced through ^{247}Cm β decay, ^{251}Es α decay and the ^{246}Bk (n,γ) reaction. In the transmutation research, however, we have to consider the production path through the ^{248}Bk(n,2n) reaction because higher energy neutrons will be used in the transmutation. Therefore, the data of ^{247}Bk were evaluated in the present work. The evaluation work for ^{247}Cm and ^{247}Bk is described in Chapter 2 and 3, respectively.

2. Evaluation of ^{247}Cm Nuclear Data

2.1 Review of Previous Evaluation

Here given is a brief review of the previous evaluation[2].

(1) Resonance region

The energy region below 60 eV was considered as the resolved resonance region. The resonance parameters were determined on the basis of experimental data by Belanova et al.[6] and Moore and Keyworth[7]. Parameters of the first resonance at 1.247 eV was adjusted so as to reproduce the thermal cross sections and resonance integrals recommended by Mughabghab[8].

In the energy region from 60 eV to 30 keV, the unresolved resonance region, the unresolved resonance parameters were obtained from the s-wave neutron strength function and an average resonance spacing recommended by Mughabghab, and p- and d-wave neutron strength functions calculated with a statistical model code CASTHY[9]. Average fission widths were adjusted so as to reproduce well the fission cross-section data measured by Moore and Keyworth.

(2) Cross-sections data above the resonance region

The fission cross section was based on the experimental data of Moore and Keyworth[7] and Fomushkin et al.[10] Large discrepancies among these two data sets were found in the energy range of 300 keV to 3 MeV. Since the tendency of large experimental values in the MeV region has been found in the experimental data of Moore and Keyworth in our evaluation work on ^{245}Cm[2] and their data of about 3.2 barns around 1.5 MeV were too large comparing with the compound nucleus formation cross section calculated with CASTHY, the data of Fomushkin et al. which are smaller than Moore and Keyworth were adopted above 300 keV. Above 3 MeV, the reliability of the previous evaluation[2] was low because no experimental data were available and the previous evaluation were made by eye-guide.

The other cross sections were calculated with CASTHY. Table 2.1 shows the excited level data considered in the calculation. The levels up to 520 keV had been

measured, and those above 550 keV were assumed to be overlapping. Optical potential parameters adopted were those determined to reproduce the ^{241}Am total cross section measured by Phillips and Howe[11]. The parameters[12] are as follows;

$$V_0 = 43.4 - 0.107E_n \text{ (MeV)}$$

$$W_s = 6.95 - 0.339E_n + 0.0531E_n^2 \text{ (MeV)}$$

$$V_{so} = 7.0 \text{ (MeV)}$$

$$r_0 = r_{so} = 1.282 \text{ (fm)}$$

$$r_s = 1.29 \text{ (fm)}$$

$$a = a_{so} = 0.60 \text{ (fm)}$$

$$b = 0.5 \text{ (fm)}$$

The form factor of surface absorption term is in the form of derivative Woods-Saxon type. The s-wave neutron strength function calculated from these parameters is 0.86×10^{-4} which is consistent with $(0.75\pm0.18)\times10^{-4}$ recommended by Mughabghab[8] within its quoted error. However, the positive coefficient of the second order term of the surface absorption makes problems in the energy region above 10 MeV where the compound nucleus formation cross section calculated from this parameter set is too large.

(3) Other data than cross sections

The CASTHY calculation was adopted for the angular distributions of elastically and inelastically scattered neutrons. The secondary neutrons emitted from fission, (n,2n) and (n,3n) reactions were assumed to be isotropic in the laboratory system.

The energy distributions of emitted neutrons were assumed to be in the form of evaporation spectrum. This assumption is not correct especially in the case of inelastic scattering to the overlapping levels.

The number of neutrons per fission was calculated from empirical formula of systematics analyzed by Howerton[13] and Tuttle[14], respectively for the prompt neutrons and delayed neutrons.

2.2 Reevaluation

The previous results were adopted in JENDL-3.2. After the previous evaluation, the following problems have been found by comparing the results with the recent experimental data:

1) The fission cross section in the resonance region

Figure 2.1 shows a comparison of the fission cross section with experimental data measured by Danon et al.[4] using Rensselaer Intense Neutron Spectrometer. In this figure the data of JENDL-3.2 and ENDF/B-VI[15] are broadened with experimental energy resolution. JENDL-3.2 is better than ENDF/B-VI, but still smaller than the experimental data in the energy region below several 10 eV.

2) Cross sections in the MeV region

The previous evaluation mainly adopted the results of statistical model calculation with CASTHY. However, calculation with the statistical model and/or evaporation model cannot reproduce well the cross sections in the MeV region, because the direct process is essential. Konshin[5] indicated that most of minor actinides in JENDL-3.2 had the same problem.

The present reevaluation was attempted to remove these drawbacks.

2.2.1 Resonance Parameters

Available experimental data on the resolved resonance parameters are as follows:

1) Moore and Keyworth[7]

Moore and Keyworth made the experiment by using an underground explosion and analyzed the resonance parameters from 20 to 60 eV.

2) Belanova et al.[6]

They measured transmission and analyzed the parameters below 18 eV.

3) Danon et al.[4]

By using Rensselaer Intense Neutron Spectrometer (RINS), the fission cross

section was measured in the energy region from 0.1 eV to 80 keV. Since energy resolution of RINS is not sharp enough, the resonances were analyzed only up to 18 eV.

In the present work, the previous evaluation above 20 eV which was based on the experimental data of Moore and Keyworth was adopted because the fission cross section of JENDL-3.2 is consistent with the experimental data in this energy region. Table 2.2 compares resonance parameters below 20 eV. The fission widths recommended by Mughabghab[8] were calculated on the basis of Belanova's data and assuming the capture width of 40 meV. Mughabghab's results are in very good agreement with the results of Danon et al. This fact means the data of Danon et al. are consistent with those of Belanova et al. However, the resonances at 2.9 and 4.4 eV were found in only one experiment.

In the present evaluation, both of the 2.9- and 4.4-eV resonances were adopted. The parameters at 4.4 eV were estimated from the fission area of 107 b·eV[4], s-wave neutron strength function of 0.75×10^{-4} and average level spacing of 1.4 eV[8]. This neutron strength function was calculated with CASTHY. Furthermore, a negative level at −0.3 eV was assumed. The parameters of 4.4-, 9.55- and 18.1-eV resonances were adjusted to reproduce better the measured cross section. The finally recommended parameters are given in Table 2.3, and cross-section data calculated from them are shown in Fig.2.3. Table 2.4 shows a comparison of the thermal cross sections and resonance integral.

In the energy range from 60 eV to 30 keV of the unresolved resonance region, the previous evaluation (JENDL-3.2) was adopted because the discrepancies between the data of Danon and JENDL-3.2 which was based on Moore and Keyworth were not so large.

2.2.2 Inelastic Scattering Cross Sections

The previous evaluation ignored the direct process. In the present work, therefore, the direct process was calculated with ECIS88[16] in the energy region above 600 keV. Deformed optical potential parameters determined by Lagrange and Jary[17] were adopted:

$$V_0 = 49.82 - 17(N-Z)/A - 0.3E_n, \quad a_0 = 0.63 \text{ fm}, \; r_0 = 1.26 \text{ fm}$$

$$V_{so} = 6.2, \quad a_{so} = 0.47 \text{ fm}, \; r_{so} = 1.12 \text{ fm}$$

$W_s = 5.52 - 9(N-Z)/A + 0.4E_n$, $E_n \leq 10$ MeV

$9.52 - 9(N-Z)/A$, $E_n \geq 10$ MeV

$a_s = 0.52$ fm, $r_s = 1.26$ fm

$\beta_2 = 0.204$, $\beta_4 = 0.051$

This set of parameters was determined by the data of $^{240, 242}$Pu in the energy range from 10 keV to 20 MeV. Table 2.5 shows energies, spin and parity of excited levels were taken from the recommendation made by Akovali[18]. Coupling between levels was considered up to the third level. The levels above 309 keV were assumed to be overlapping.

The cross section of compound nucleus process was calculated with CASTHY. Spherical optical potential parameters used for the real term (V_0), spin-orbit term (V_{so}) and surface absorption term (W_s) are as follows:

$V_0 = 45.036 - 0.3E_n$, $a_0 = 0.626$ fm, $r_0 = 1.256$ fm

$V_{so} = 7.5$, $a_{so} = 0.626$ fm, $r_{so} = 1.256$ fm

$W_s = 4.115 + 0.4E_n$, $a_s = 0.555 + 0.0045E_n$ fm

$r_s = 1.26$ fm

This set of parameters was determined by Ignatyuk et al.[19] so as to reproduce the compound nucleus formation cross section calculated from deformed potential which was obtained by Klepatskij et al.[20] analyzing the data of ^{235}U, ^{238}U, ^{239}Pu and ^{240}Pu. The deformed potential of Klepatskij et al. is almost the same as that of Lagrange and Jary. This set of spherical potential parameters has the same problem as that used in the previous evaluation: the surface absorption term becomes larger and larger at high energies, then the compound formation cross section is overestimated in the high energy region. The calculated inelastic scattering cross section to the overlapping levels was too large at the energies above 12 MeV in the case of ^{247}Cm, and modified by eye-guiding to smaller values. In the reference of 19, the surface absorption term was written as $W_D = 4.115-0.4E$. However, the sign of 0.4 must be '+' comparing with the deformed potential.

The finally recommended inelastic scattering cross sections were obtained as a sum of ECIS88 and CASTHY calculations.

2.2.3 (n,2n), (n,3n) and (n,4n) Reaction Cross Sections

For the (n,2n) and (n,3n) reaction cross sections, Konshin's calculations[5] with the STAPRE code[21] based on Hauser-Feshbach statistical model and pre-equilibrium model were adopted. The (n,4n) reaction cross section was taken from JENDL-3.2, because its threshold energy is very high and the cross section might be unimportant.

2.2.4 Fission Cross Section

Figure 2.3 shows the fission cross section above 100 keV. Konshin's calculation[5] is in good agreement with experimental data of Fomushkin et al.[10] around 3 MeV, but larger than the experimental data in the energy range below 3 MeV, and disagreement with new experimental data measured by Fomushkin et al.[22] at 14 MeV. On the other hand, JENDL-3.2 reproduces well the data of Fumushkin et al. below 3 MeV and is in good agreement with the new experiment at 14 MeV. Therefore, the previous evaluation (JENDL-3.2) was adopted after correcting the data above 11 MeV to reproduce better the new Fomushkin's data.

2.2.5 Other Cross Sections

(1) Total cross section

CASTHY calculation was adopted.

(2) Capture cross section

The capture cross section was given as a sum of CASTHY calculation and direct capture cross section calculated from the simple formula proposed by Benzi and Reffo[23]. An average radiative capture width of 40 meV and an average level spacing of 1.4 eV[8] were assumed in the calculation. The direct capture cross section was normalized to 1.0 mb at 14 MeV.

(3) Elastic scattering cross section

The elastic scattering cross section was calculated by subtracting a sum of partial cross sections from the total cross section.

2.2.6 Other Data

(1) Angular distributions of elastically scattered neutrons

ECIS88 calculation was adopted in the energy region above 600 keV. Since no calculation was made below 600 keV with ECIS88, the distributions were assumed to be the same as the previous evaluation.

(2) Angular distributions of inelastically scattered neutrons

The angular distributions of inelastically scattered neutrons from 1st, 2nd and 3rd levels were a sum of those of direct neutrons calculated with ECIS88 and compound neutrons with CASTHY. For the other levels, CASTHY calculations were adopted.

(3) Angular distributions of neutrons emitted from (n,2n), (n,3n), (n,4n) reactions and fission

All of them were assumed to be isotropic in the laboratory system.

(4) Energy distributions of neutrons emitted from (n,2n), (n,3n), (n,4n) reactions and fission

Konshin's calculation with STAPRE was adopted to the energy distributions of neutrons emitted from (n,2n) and (n,3n) reactions. Therefore, the evaporation spectra adopted in the previous evaluation were improved with the precompound spectra.

The previous evaluation was adopted for the (n,4n) reaction and fission neutrons. The previous evaluation gave evaporation spectrum with nuclear temperature estimated from level density parameters for the (n,4n) reaction and from systematics reported by Smith et al.[24] for the fission neutrons.

(5) Number of neutrons per fission

The previous evaluation was adopted;

$$\nu_p = 3.79 + 0.207E_n(\mathrm{MeV})$$

$$\nu_d = 0.0134 \qquad E_n \leq 6\ \mathrm{MeV}$$

0.00916 $E_n \geq 8$ MeV

The constant term of number of prompt neutrons (ν_p) was taken from Zhuravlev et al.[25] The coefficient of first order term was based on Howerton's systematics.[13] The number of delayed neutrons (ν_d) was calculated from Tuttle's systematics[14]. The ν_d in the energy range from 6 to 8 MeV was linearly interpolated from these two values.

2.3 Conclusion

Cross sections recommended in the present work are shown in Figs. 2.4 to 2.9 comparing with the previous evaluation (JENDL-3.2) and ENDF/B-VI. The cross sections in the resolved resonance region are averaged in the 1/4 lethargy intervals. Actual data in this energy region given in a data file are represented with the resolved resonance parameters given in Table 2.3.

Improvement from the previous evaluation was made especially to the fission cross section below about 50 eV, the inelastic scattering cross sections above 1 MeV, and the (n,2n) and (n,3n) reaction cross sections. Large discrepancies are found among the cross-section data in ENDF/B-VI and the present work. At least, the experimental fission cross sections are reproduced better by the present work.

3. Evaluation of ^{247}Bk Nuclear Data

Neither evaluated nuclear data nor any experimental data are exist for ^{247}Bk. Therefore, the present evaluation was based on theoretical calculations and systematics of data.

3.1 Thermal cross sections

It is very difficult to find out systematics on cross sections at the thermal neutron energy, because the thermal cross sections are affected by several resonances around the thermal energy, especially the position of the nearest resonance. In the present work, however, we could not help considering systematics of the thermal cross sections because there were no experimental data.

In the case of even neutron nuclides such as ^{247}Bk, the fission is a sub-threshold reaction, and its cross section is very small. Comparisons of measured thermal fission cross sections[8,26] of nuclides ranging from Pa to Cf are made in Figs.3.1 and 3.2. The horizontal axis of Fig. 3.1 is fission threshold energies, and that of Fig. 3.2 values of Z^2/A where Z and A is an atomic number and a mass number, respectively. The fission threshold energies were calculated from the following equation used by Howerton[13]:

$$E_{th}(Z,A) = 18.6 - 0.36Z^2/(A+1) + 0.2[2-(-1)^{A+1+Z} - (-1)^Z] - B_n \quad \text{(MeV)}$$

where B_n stands for a neutron separation energy from the compound nuclide with a mass number of A+1. From these figures, it is seen that the fission cross section becomes smaller with the threshold energies, and rapidly larger with Z^2/A, except for the case of Cm isotopes. From these figures, the thermal fission cross section of ^{247}Bk with the threshold energy of 0.284 MeV and Z^2/A of 37.94 was estimated to be in the range from several tens to several hundreds barns. We assumed the fission cross section of 100 barns.

The thermal capture cross sections[8,26] of even-neutron mass nuclides is shown in Fig. 3.3. The horizontal axis is reaction Q values. It is roughly seen that the capture cross section becomes larger with Q values. The capture cross section of ^{247}Bk at the thermal energy was very roughly estimated to be 200 barns because of its Q value of 5.46 MeV.

3.2 Resonance Parameters

The resolved resonance parameters were determined so as to reproduce the above-mentioned thermal cross sections, by considering also the s-wave neutron strength function (S_0) of 1.0×10^{-4}, average level spacing (D) of 2.01 eV, radiative capture width (Γ_γ)of 26 meV and fission width (Γ_f) of 13 meV. S_0 was estimated from its systematic trends[8], and D was calculated from level density parameters described in the next section (Table 3.2). Γ_γ was calculated from a sytematics given by Malecki et al.[27] Γ_f was obtained from a ratio of the fission and capture cross sections at the thermal energy and the capture width. The scattering radius of 9.27 fm was obtained from spherical optical model calculation with CASTHY.

The upper boundary of the resolved resonance region was selected to be 150 eV. No unresolved resonance region was considered.

3.3 Cross Sections above Resonance Region

(1) Total cross section

The total cross section was calculated with CASTHY using the spherical optical potential parameters of Ignatyuk et al. mentioned in Chapter 2, except for the energy region below about 2 keV where adopted cross section was a sum of partial cross sections, and a little larger than the CASTHY calculation because of modification of the elastic scattering cross section.

(2) Fission cross section

In the energy region above 1 keV, adopted was the cross-section data calculated by Konshin[5] with STAPRE. Below 1 keV, the cross section was determined by eye-guide to connect smoothly to the average values in the resonance region. Average fission cross section around 150 eV was about 10 barns. The shape of cross section was assumed to go down with the incident energy and to connect to Konshin's calculation of 0.2 barn at 1 MeV.

(3) (n,2n) and (n,3n) reaction cross sections

Konshin's calculation[5] was adopted.

(4) Inelastic scattering cross sections

Table 3.1 shows adopted levels which was evaluated by Schmorak[28]. The levels above 983 keV were assumed to be overlapping. Contributions from the direct process were calculated with ECIS88 for the 29.9-, 71.6- and 125.5-keV levels. The deformed optical potential parameters used in the present work were the same as those of Lagrange and Jary[17] listed in Chapter 2. The cross sections of compound process were calculated with CASTHY. Table 3.2 shows level density parameters used in the calculation, which were determined to be consistent with the number of excited levels and the systematic trend of level density parameters. Finally adopted cross sections are a sum of the both calculations.

(5) Capture cross section

Adopted cross section was a sum of CASTHY calculation and direct capture cross section calculated from Benzi-Reffo's formula. The capture width of 26 meV and average level spacing of 2.01 eV which were consistent with the resolved resonance region were assumed in the CASTHY calculation.

(6) Elastic scattering cross section

The elastic scattering cross section was estimated by subtracting a sum of partial cross sections from the total cross section in the energy region above 2 keV. Since the values obtained by the subtraction were too small below several keV, the constant value of 1.19 barns calculated with CASTHY at 2 keV was adopted below 2 keV.

3.4 Angular Distributions of Emitted Neutrons

The angular distributions of elastically and inelastically scattered neutrons were determined on the basis of ECIS88 and CASTHY calculations. Those of the (n,2n) and (n,3n) reactions and fission were assumed to be isotropic in the laboratory system.

3.5 Energy Distributions of Emitted Neutrons

Konshin's calculation[5] with STAPRE was adopted to the energy distributions of neutrons emitted from (n,2n) and (n,3n) reactions. The evaporation spectra was assumed

to the fission neutrons and temperature of 1.44 MeV was estimated from the systematics of Smith et al.[24)]

3.6 Number of Neutrons per Fission

The number of prompt neutrons (ν_p) was based on Howerton's systematics[13)] and that of delayed neutrons (ν_d) Tuttle's systematics[14)]:

$$\nu_p = 3.5025 + 0.202E_n(\mathrm{MeV})$$

$$\nu_d = 0.004198 \qquad E_n \leq 6\ \mathrm{MeV}$$

$$0.002903 \qquad E_n \geq 8\ \mathrm{MeV}$$

3.7 Conclusion

The present results are shown in Figs. 3.4 to 3.9. The cross sections in the resolved resonance region below 150 eV are averaged in the 1/4 lethargy intervals.

Acknowledgment

The authors thank Dr. K. Shibata of Nuclear Data Center, JAERI, for his careful reading of this manuscript and valuable comments.

References

1) T. Nakagawa, T. Fukahori, S. Chiba and Y. Kikuchi: *Proc. Intern. Conf. and Technol. Exposition on Future Nuclear Systems: Emerging Fuel Cycles and Waste Disposal Options GLOBAL 93*, Seattle, USA, Sep. 12–17, 1993, p.467 (1993).
2) T. Nakagawa: "Evaluation of Neutron Nuclear Data for Curium Isotopes," *JAERI-M* 90-101 (1990).
3) T. Nakagawa, K. Shibata, S. Chiba, T. Fukahori, Y. Nakajima, Y. Kikuchi, T. Kawano, Y. Kanda, T. Ohsawa, H. Matsunobu, M. Kawai, A. Zukeran, T. Watanabe, S. Igarasi, K. Kosako and T. Asami: *J. Nucl. Sci. Technol.*, **32**, 1259 (1995).
4) Y. Danon, R.E. Slovacek and R.C. Block: *Nucl. Sci. Eng.*, **109**, 341 (1991).
5) V.A. Konshin: "Consistent Calculations of Fast Neutron Induced Fission, (n,2n) and (n,3n) Cross-Sections for 71 Isotopes of Th, Pa, U, Np, Pu, Am, Cm, Bk and Cf," *JAERI-Research* 95-010 (1995).
6) T.B. Belanova, A.G. Kolesov, A.V. Klinov, S.N. Nikol'skii,V.A. Poruchikov, V.N. Nefedov, V.S. Artamonov, R.N. Ivanov and S.M. Kalebin: *Sov. Atomic Energy*, **47**, 772 (1979).
7) M.S. Moore and G.A. Keyworth: *Phys. Rev.*, **C3**, 1656 (1971).
8) S.F. Mughabghab: "Neutron Cross Sections, Vol. 1, Neutron Resonance Parameters and Thermal Cross Sections, Part B: Z=61–100," Academic Press, Inc. (1984).
9) S. Igarasi and T. Fukahori: "Program CASTHY – Statistical Model Calculation for Neutron Cross Sections and Gamma Ray Spectrum –," *JAERI* 1321 (1991).

10) E.F. Fomushkin, G.F. Novoselov, Yu.I. Vinogradov, V.V. Gavrilov and V.A. Zherebtsov: *Sov. Atomic Energy*, **62**, 340 (1987).

11) T.W. Phillips and R.E. Howe: *Nucl. Sci. Eng.*, **69**, 375 (1979).

12) S. Igarasi and T. Nakagawa: "Evaluation of Neutron Nuclear Data for ^{242}Cm," *JAERI-M* 8342 (1979) [in Japanese].

13) R.J. Howerton: *Nucl. Sci. Eng.*, **62**, 438 (1977).

14) R.J. Tuttle: Proc. Consultants' Meeting on Delayed Neutron Properties, Vienna, 1979, *INDC(NDS)-107/G+Special*, p.29 (1979).

15) R.W. Benjamin, K.W. MacMurdo and R.J. Howerton: ENDF/B-VI, MAT=9646 (1976).

16) J. Raynal: "Coupled Channel Calculation and Computer Code ECIS," program package NEA 0850/08 available from OECD NEA Data Bank.

17) Ch. Lagrange and J.Jary: *NEANDC(E)* 198 "L" (1978).

18) Y.A. Akovali: *Nucl. Data Sheets*, **66**, 505 (1992).

19) A.V. Ignatyuk, A.B. Klepatskij, V.M. Maslov and E.Sh. Sukhovitskij: *Sov. J. Nucl. Phys.*, **42**, 360 (1985).

20) A.B. Klepatskij, V.A. Konshin and E.Sh. Sukhovitskij: *INDC(CCP)*-161/L (1981).

21) M. Uhl and B. Strohmaier: *IRK*-76/01 (1976).

22) E.F. Fomushkin, G.F. Novoselov, V.V. Gavrilov and Ju.I. Vinogradov: *Proc. Intern. Conf. On Nuclear Data for Science and Technology*, Jülich, Germany, 13–17 May 1991, p.439 (1991).

23) V. Benzi and G. Reffo: *CCDN-NW*/10 (1969).

24) A.Smith, G.Guenther, G.Winkler and R.Mcknight: "Prompt-Fission-Neutron Spectra of ^{233}U, ^{235}U, ^{239}Pu and ^{240}Pu Relative to that of ^{252}Cf," *ANL/NDM*-50 (1979).

25) K.D. Zhuravlev, Yu.S. Zamyatnin, N.I. Kroshkin: *Proc. 2nd All Union Conf. Neutron Physics*, Kief, 1973, Vol.4, p.57 (1973) [in Russian]

26) http://www.nndc.bnl.gov/nndc/nudat/xriform.html, Brookhaven National Laboratory, National Nuclear Data Center, USA (July 4, 1997).

27) H. Malecki, A.B. Popov and K. Tshezak: *Yad. Fiz.*, **37**, 284 (1983).

28) M.R. Schmorak: *Nucl. Data Sheets*, **59**, 507 (1990).

29) V.D. Gavrilov and V.A. Goncharov: *Sov. Atomic Energy*, **44**, 274 (1978).

30) J. Halperin, H.H. Oliver and R.W. Stoughton: "The Fission Thermal-Neutron Cross Section and Resonance Integral of ^{245}Cm, ^{247}Cm and ^{249}Cf," *ORNL*-4581, p.37 (1970).

31) R.W. Benjamin, K.W. MacMurdo and J.D. Spencer: *Nucl. Sci. Eng.*, **47**, 203 (1972).

32) K.D. Zhuravlev, N.I. Kroshkin and A.D. Chetverikov: *Sov. Atomic Energy*, **39**, 907 (1976).

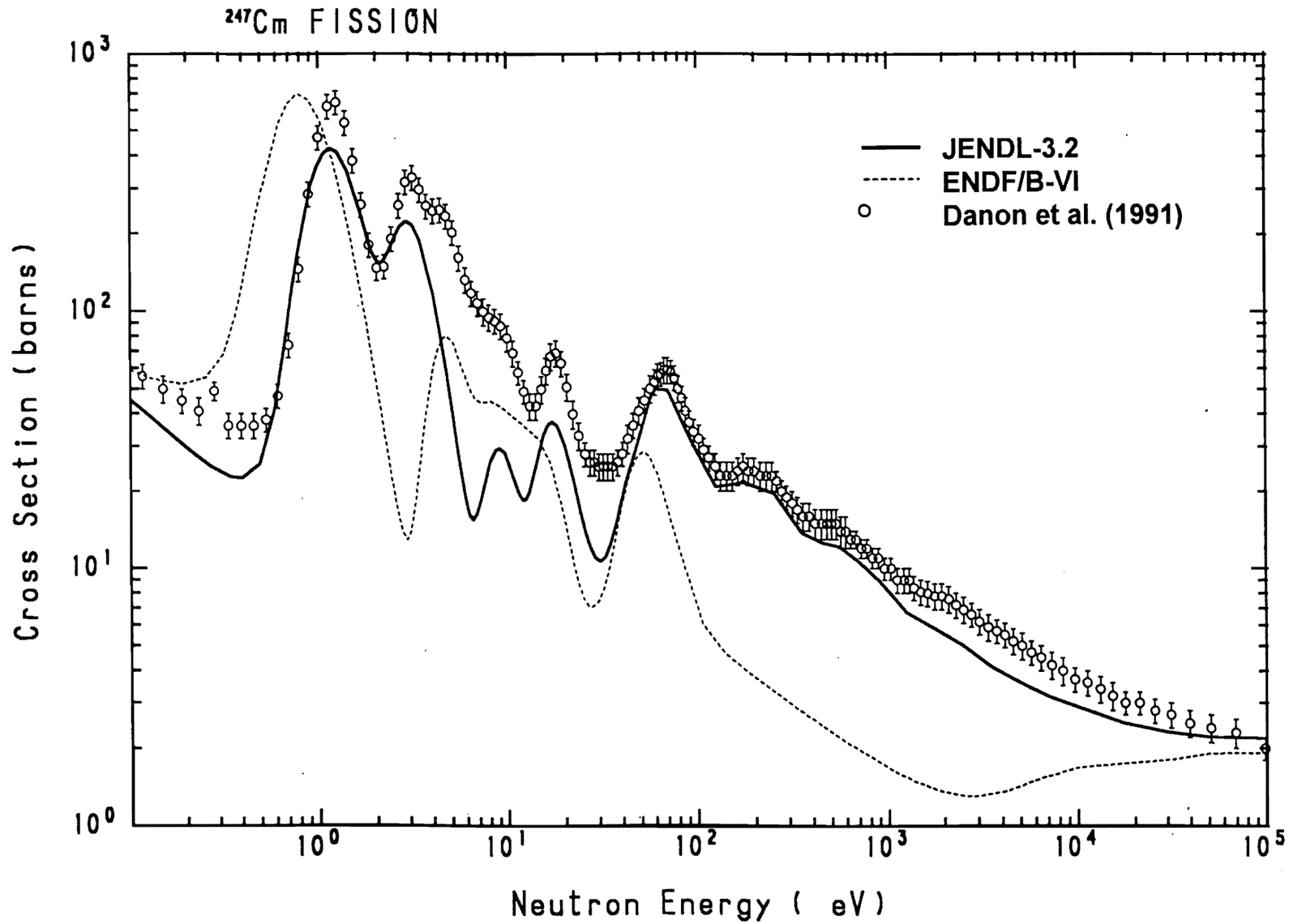

Fig. 2.1 Comparison of Fission Cross Sections (JENDL-3.2, ENDF/B-VI and Danon et al.[Da91])

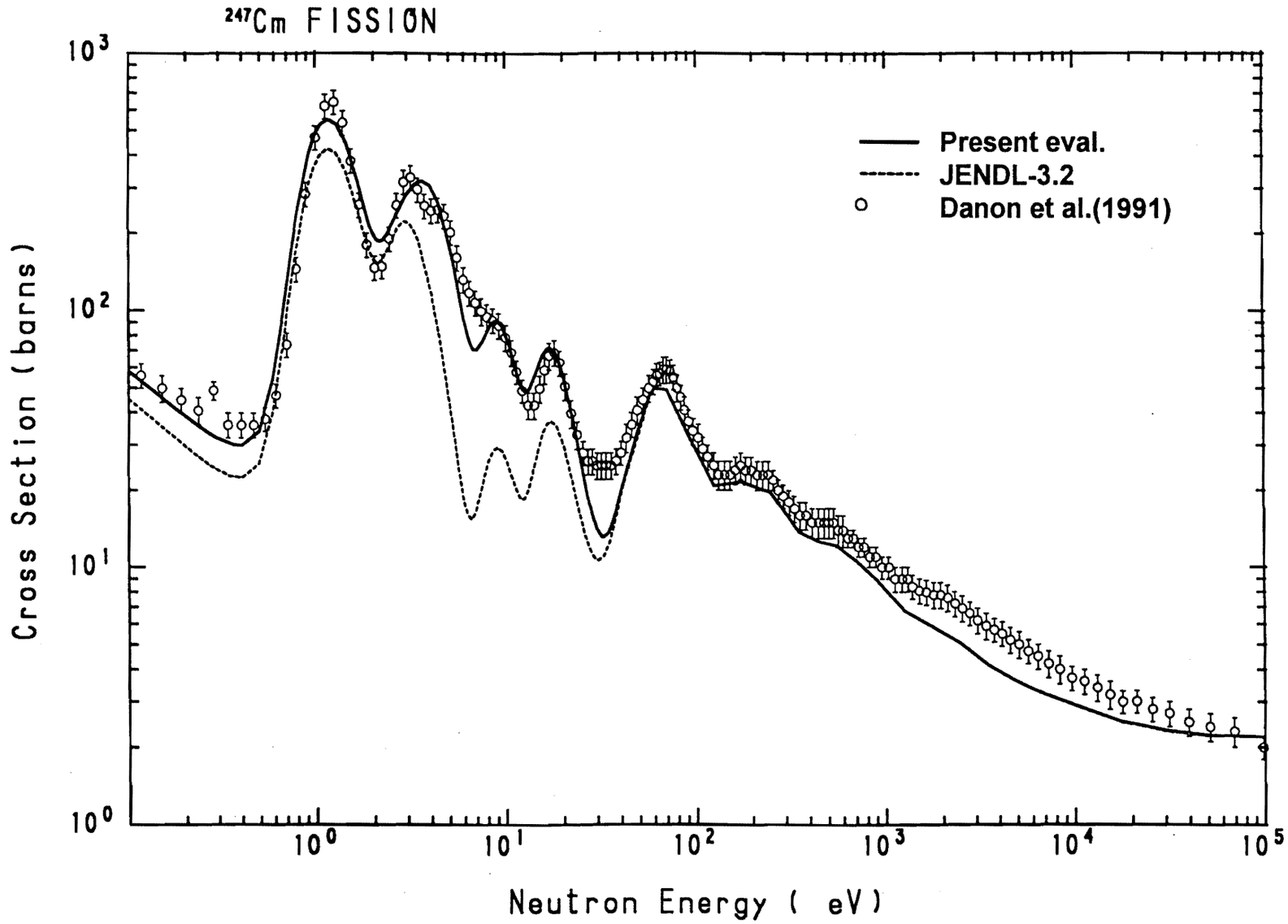

Fig. 2.2 Comparison of fission cross sections of ^{247}Cm (Present evaluation, JENDL-3.2 and Danon et al.[4])

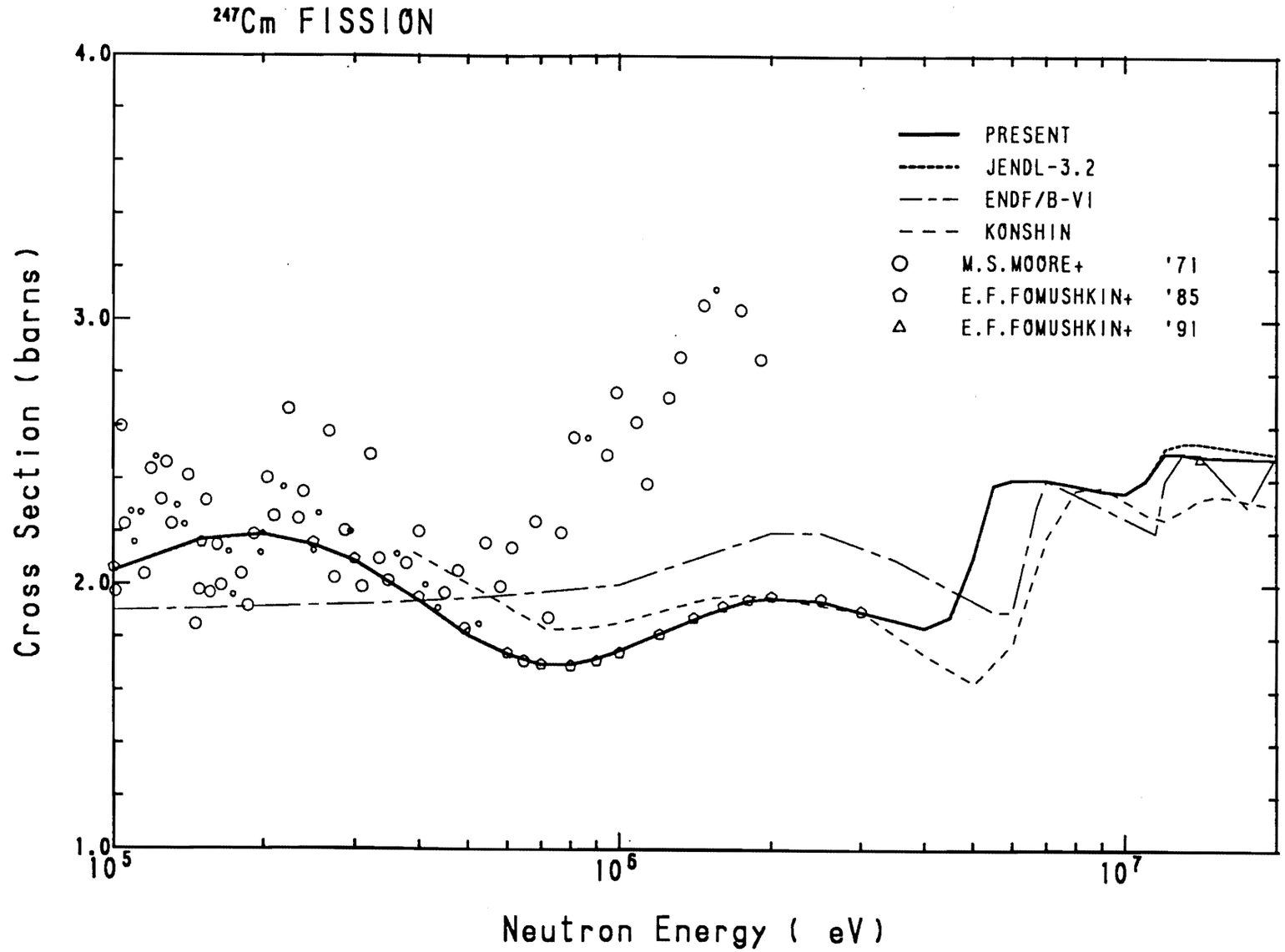

Fig. 2.3 Fission cross section of ^{247}Cm (100 keV to 20 MeV)

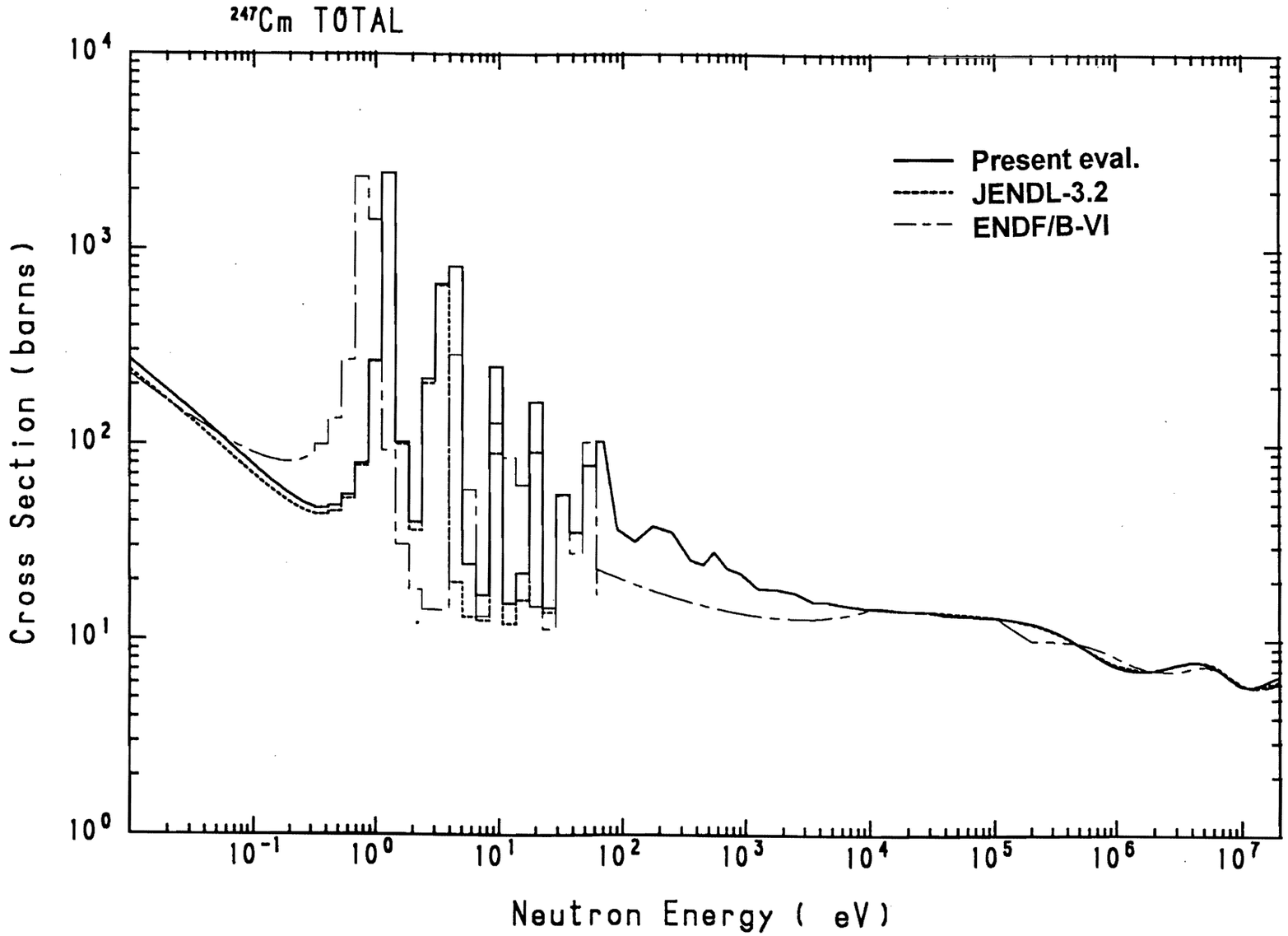

Fig. 2.4 Total cross section of ^{247}Cm

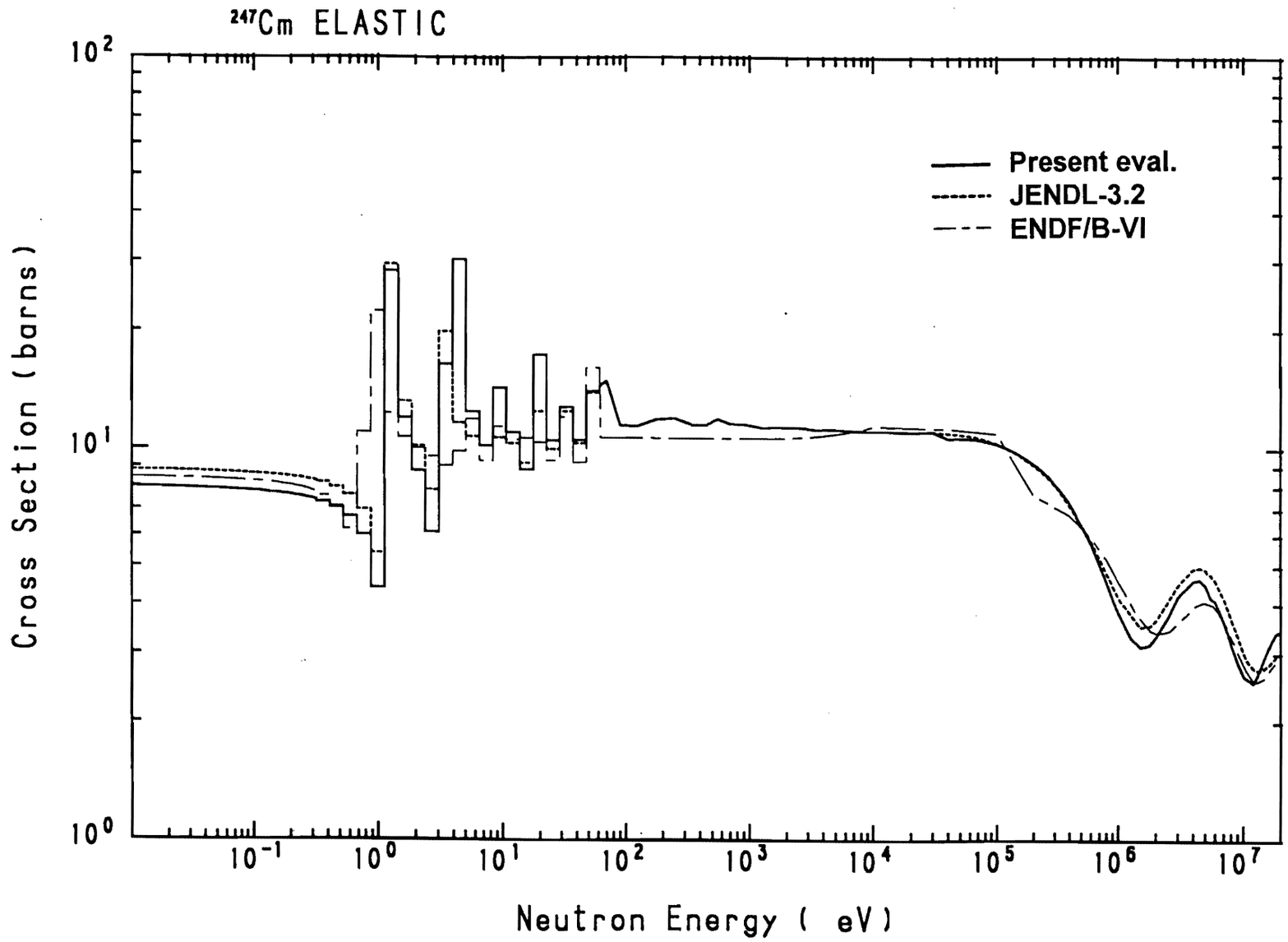

Fig. 2.5 Elastic scattering cross section of ^{247}Cm

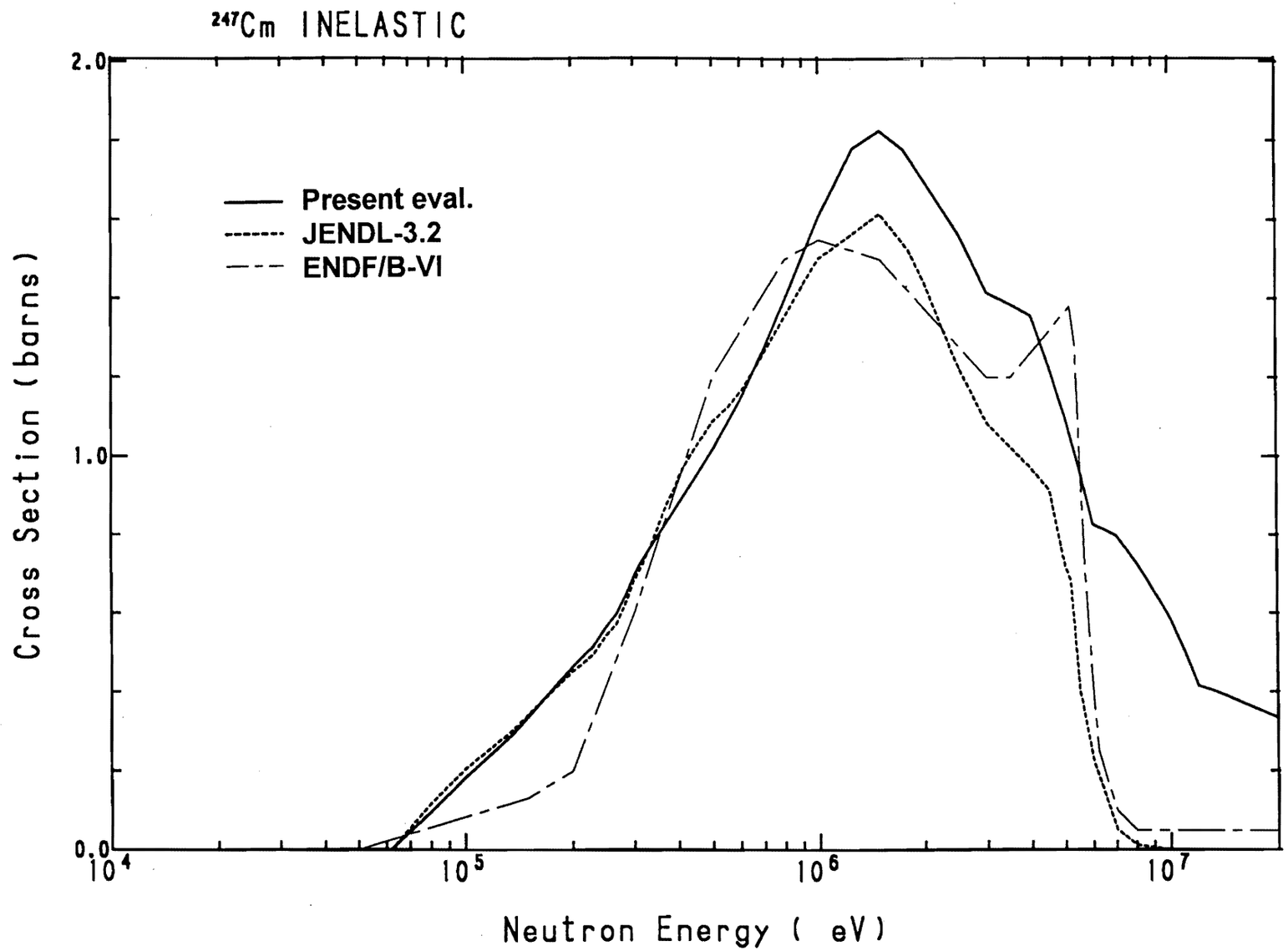

Fig. 2.6 Inelastic scatting cross section of ^{247}Cm

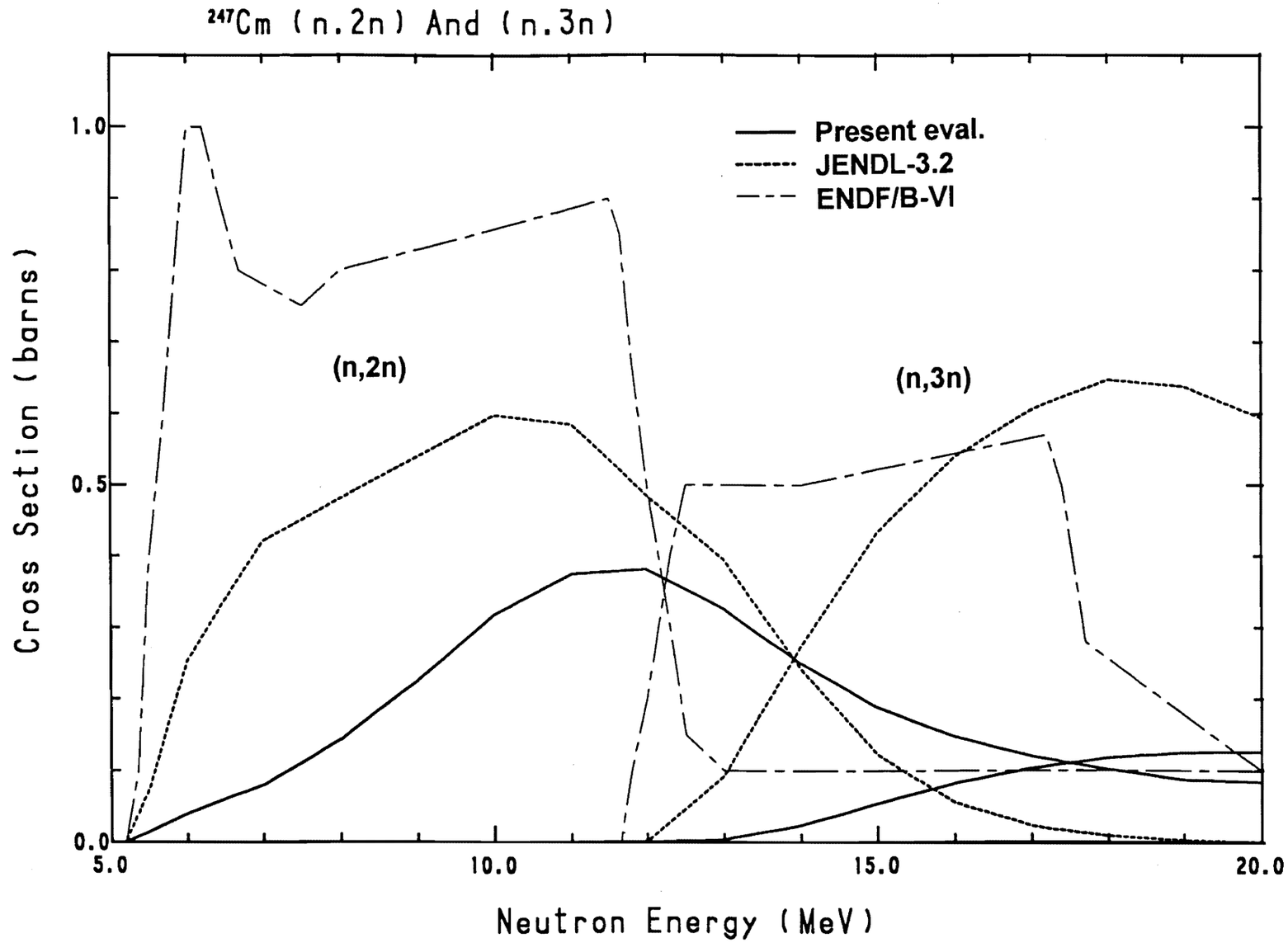

Fig. 2.7 (n,2n) and (n,3n) reaction cross sections of ^{247}Cm

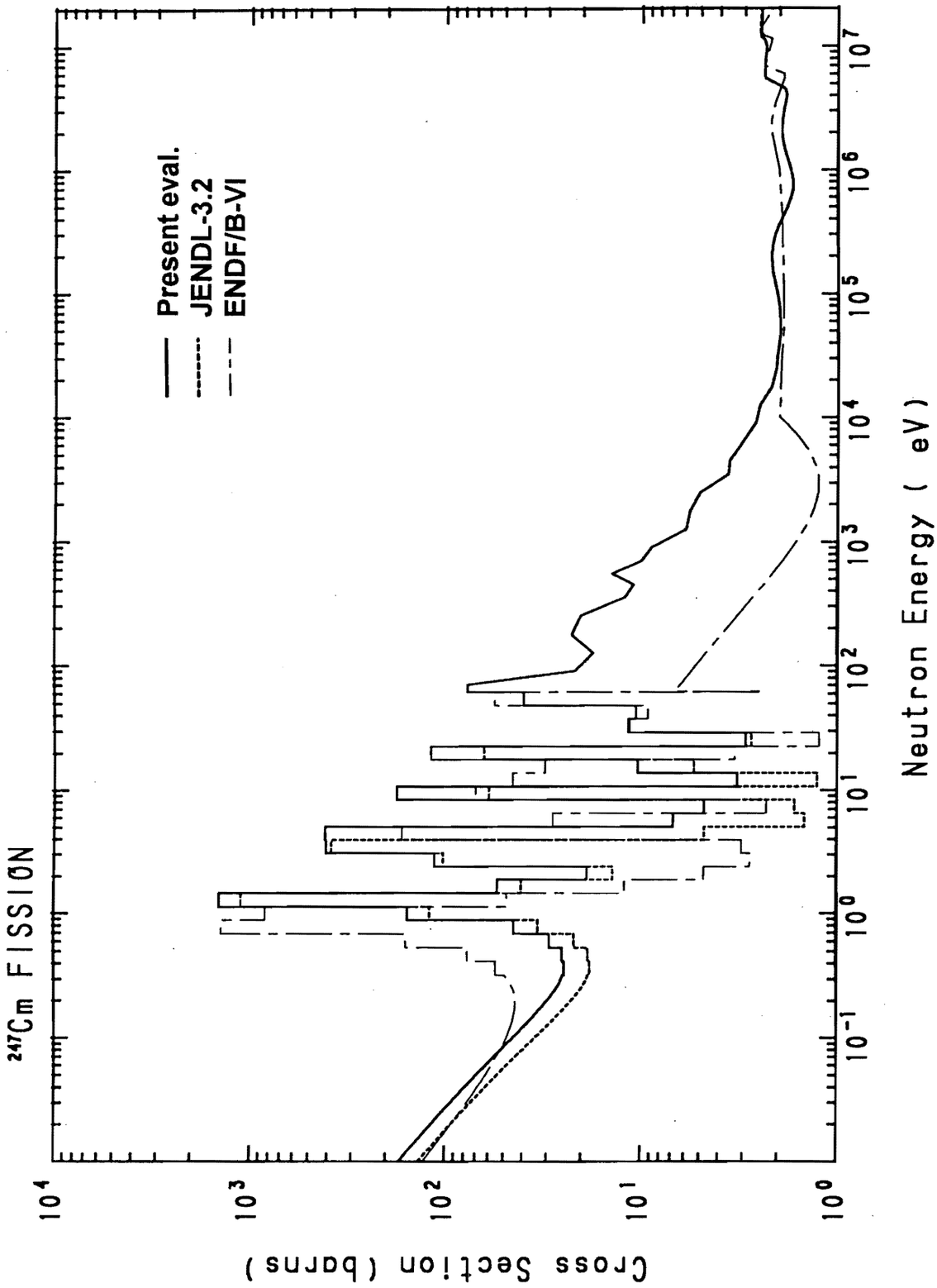

Fig. 2.8 Fission cross section of ^{247}Cm

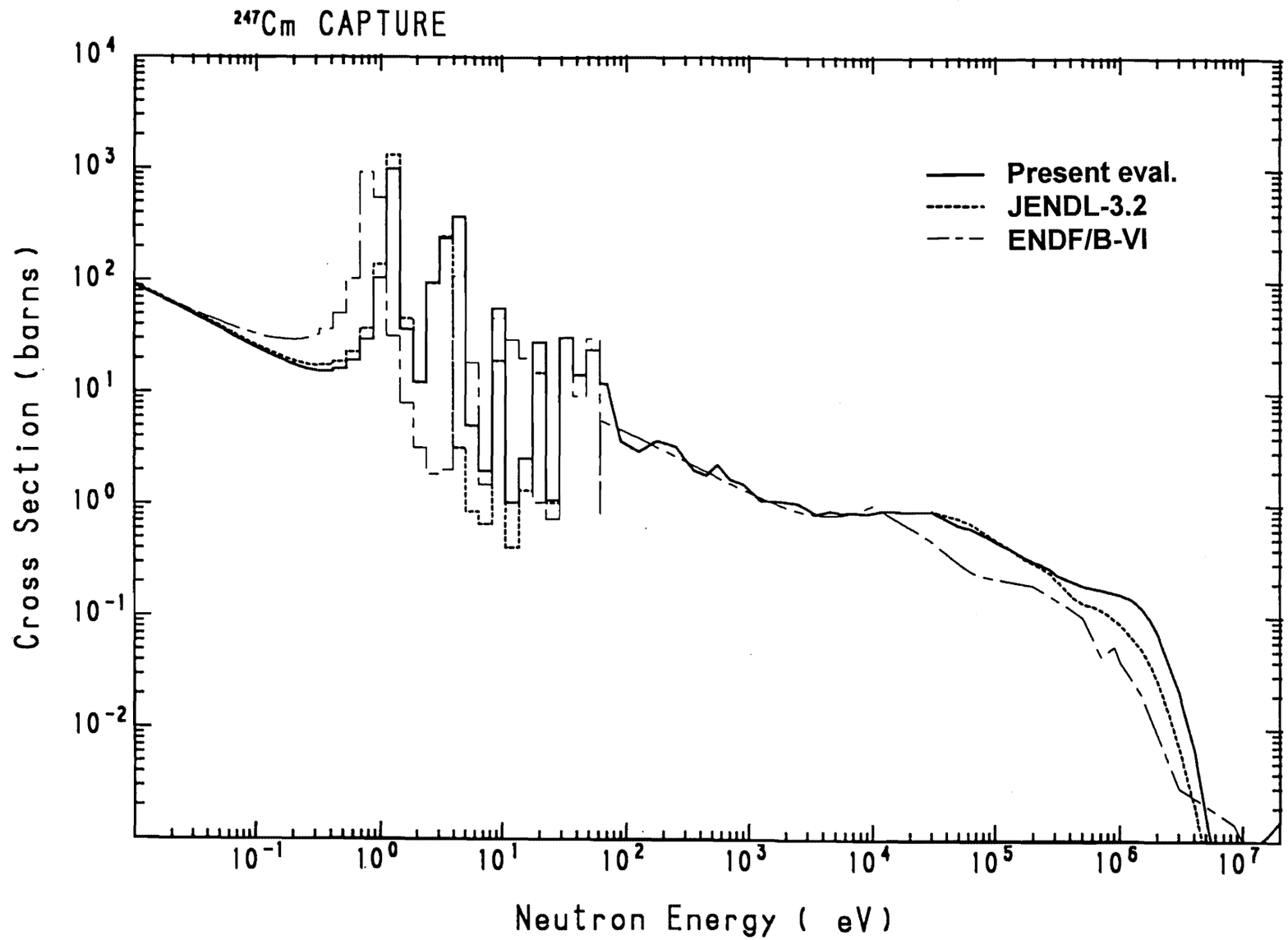

Fig. 2.9 Capture cross section of ^{247}Cm

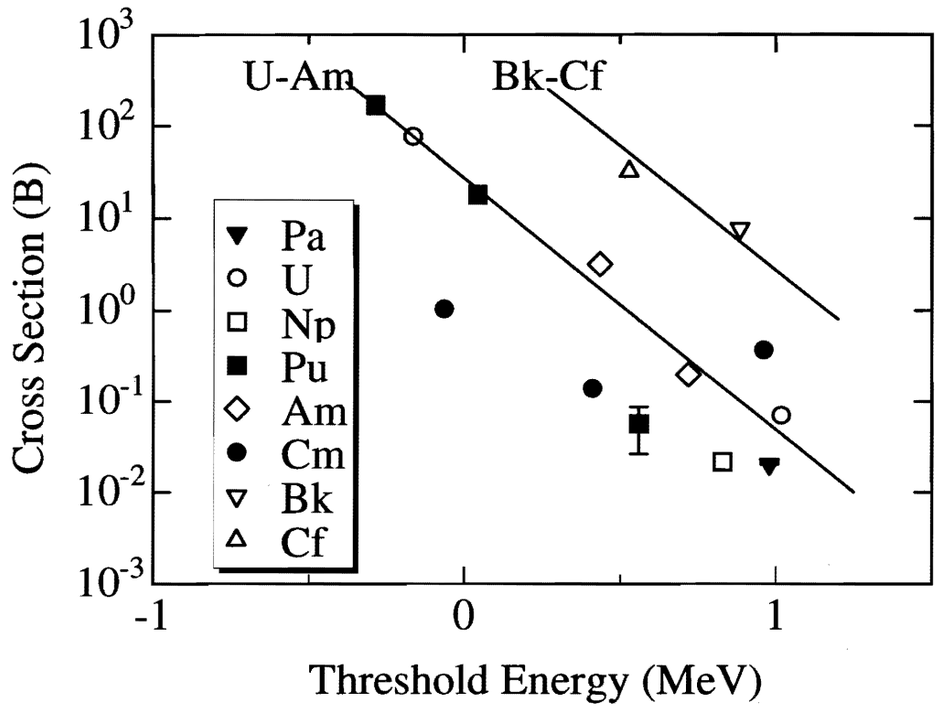

Fig. 3.1 Systematic trend of thermal fission cross sections for even-neutron nuclides. The horizontal axis is fission threshold energies. Solid lines were drawn by hand to estimate a systematic trend of cross sections.

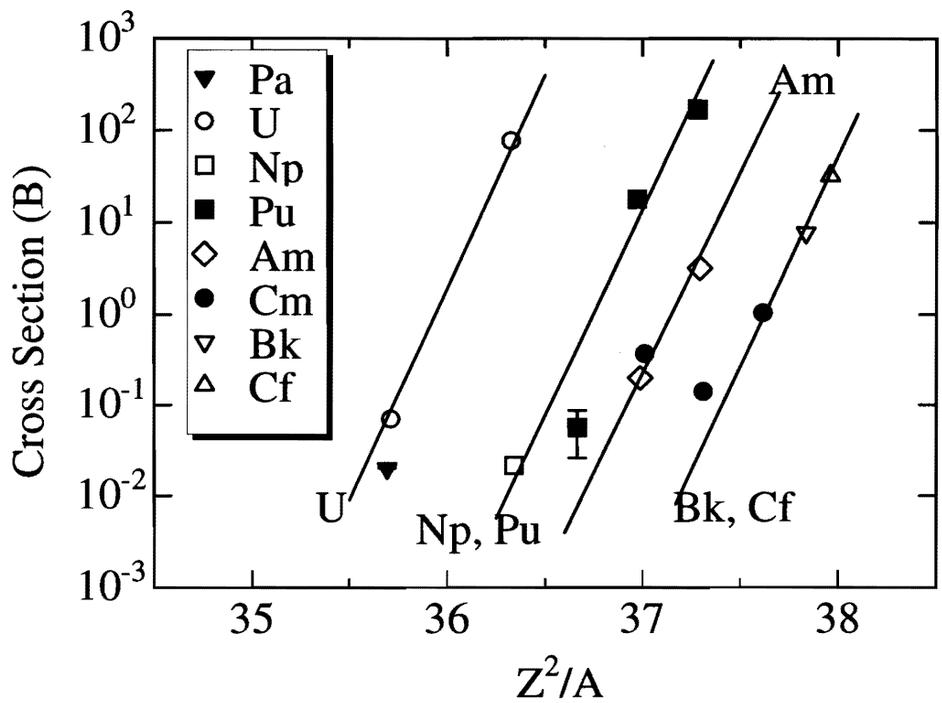

Fig. 3.2 Systematic trend of thermal fission cross sections for even-neutron nuclides. The horizontal axis is Z^2/A where Z is an atomic number and A a mass number. Solid lines were drawn by hand to estimate a systematic trend of cross sections.

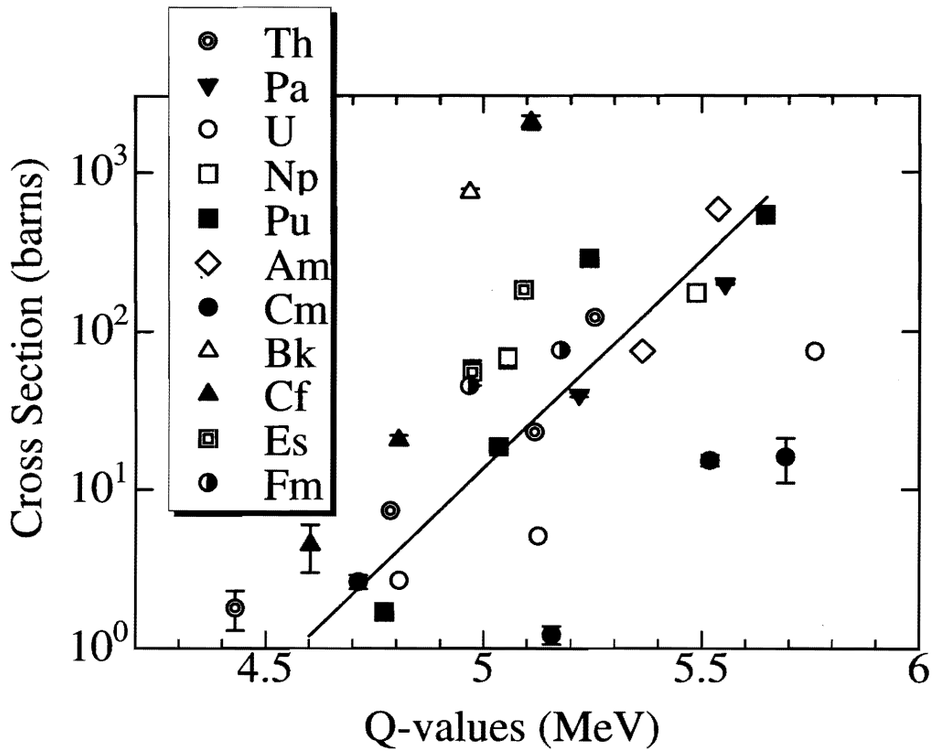

Fig. 3.3 Systematic trend of thermal capture cross sections for even-neutron nuclides. The horizontal axis is Q values of neutron capture. The solid line was roughly drawn by hand to estimate a systematic trend of cross sections.

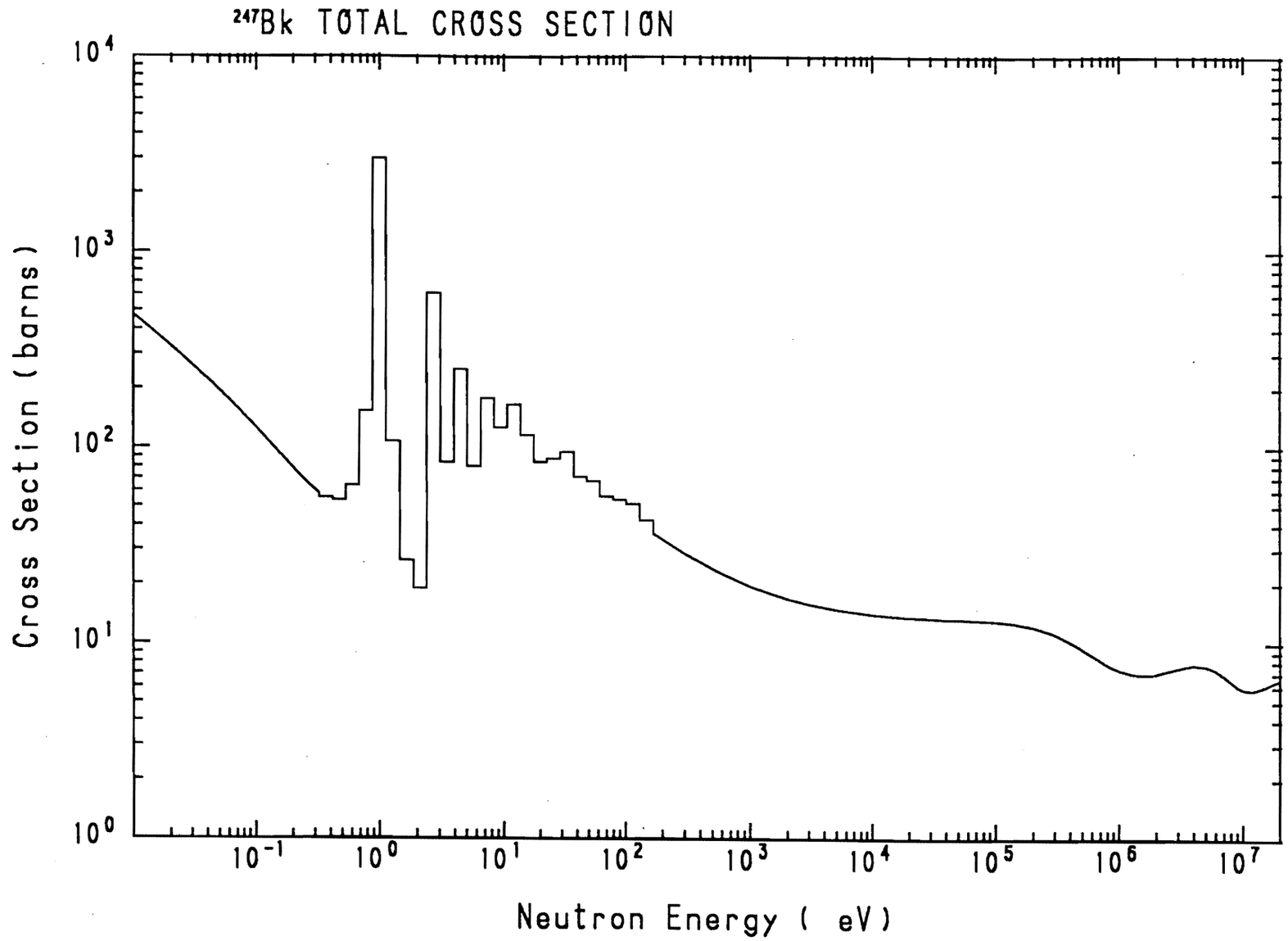

Fig. 3.4 Total cross section of ^{247}Bk

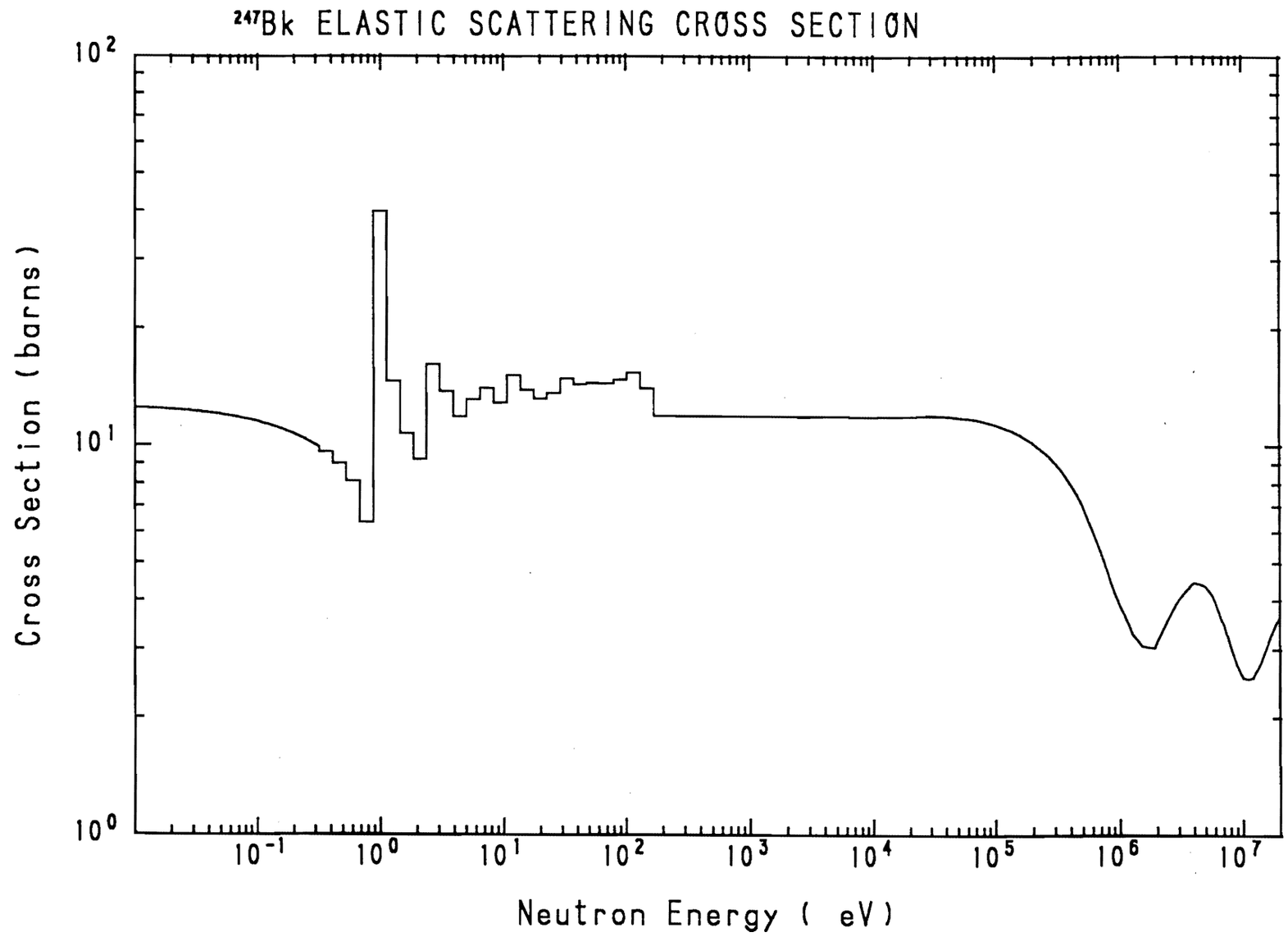

Fig. 3.5 Elastic scattering cross section of ^{247}Bk

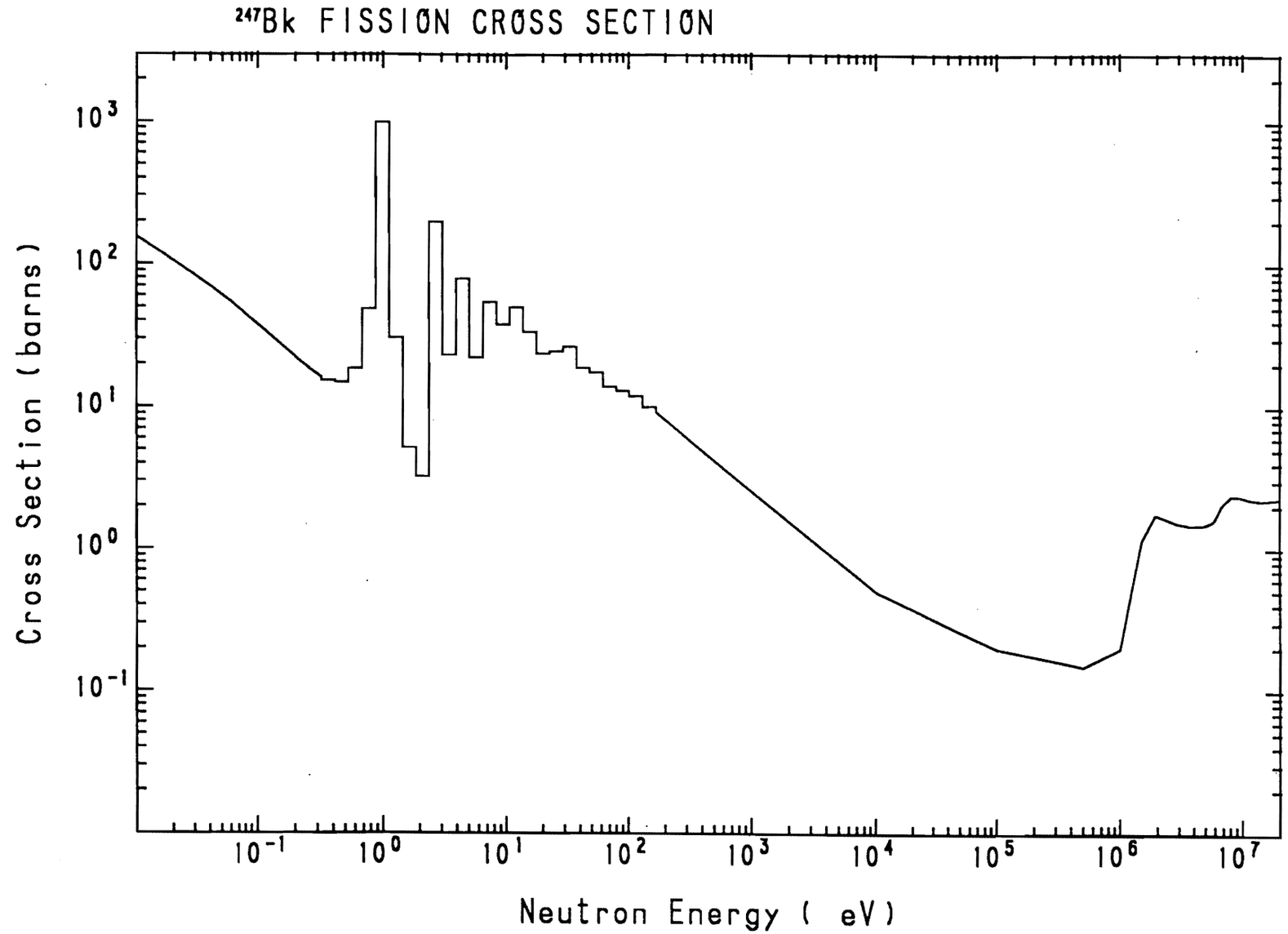

Fig. 3.6 Fission cross section of ^{247}Bk

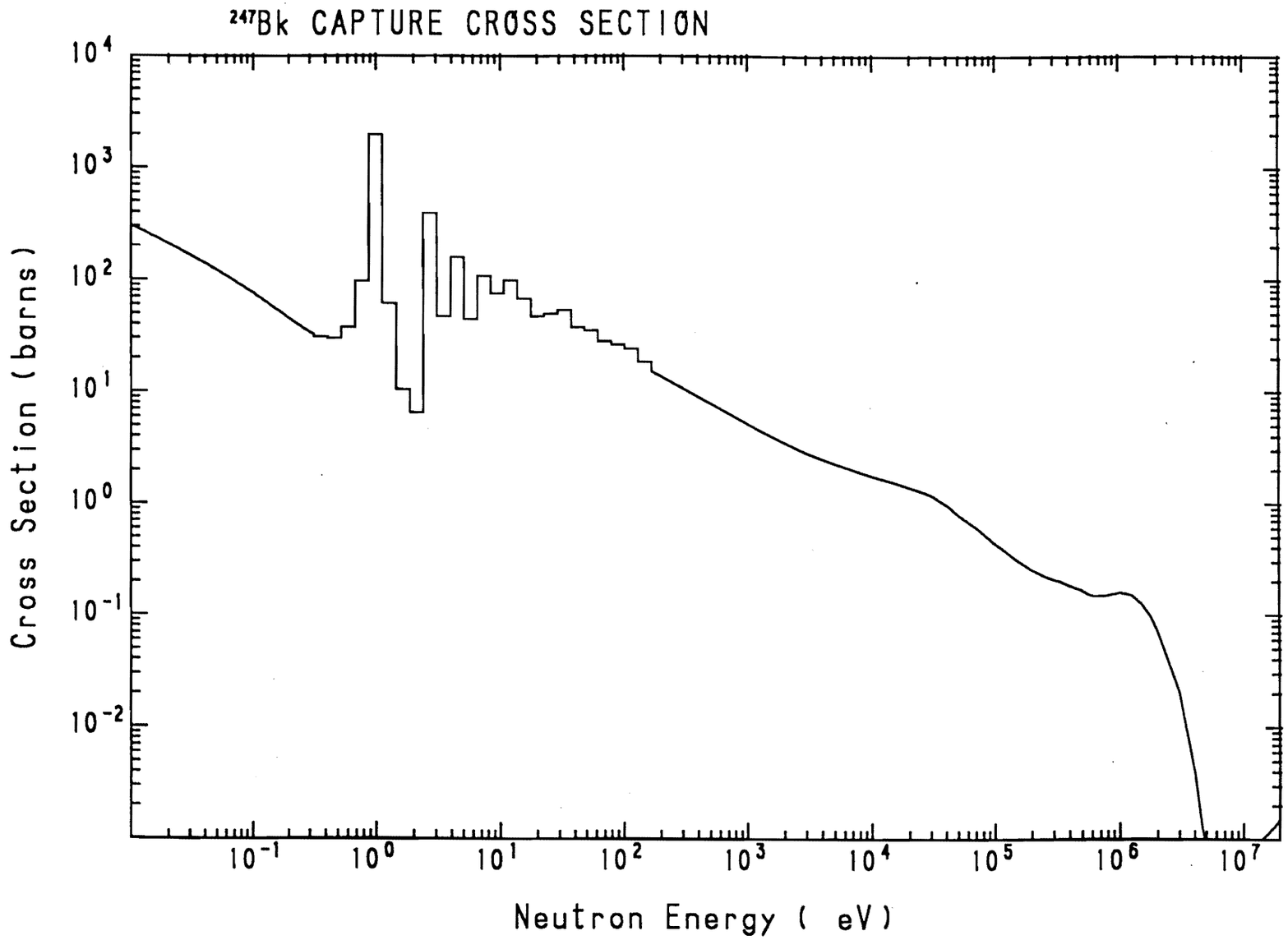

Fig. 3.7 Capture cross section of ^{247}Bk

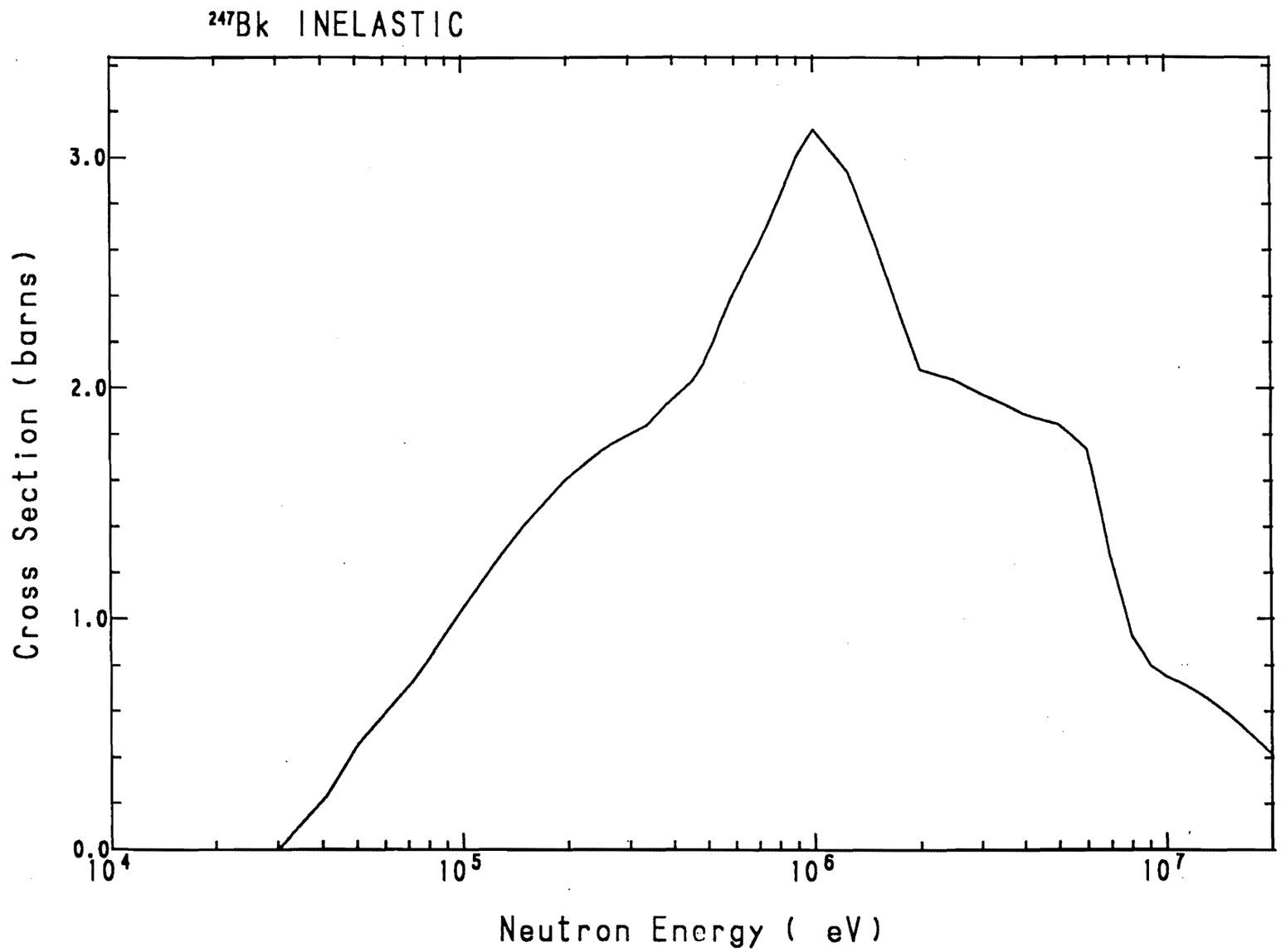

Fig. 3.8 Total inelastic scattering cross section of ^{247}Bk

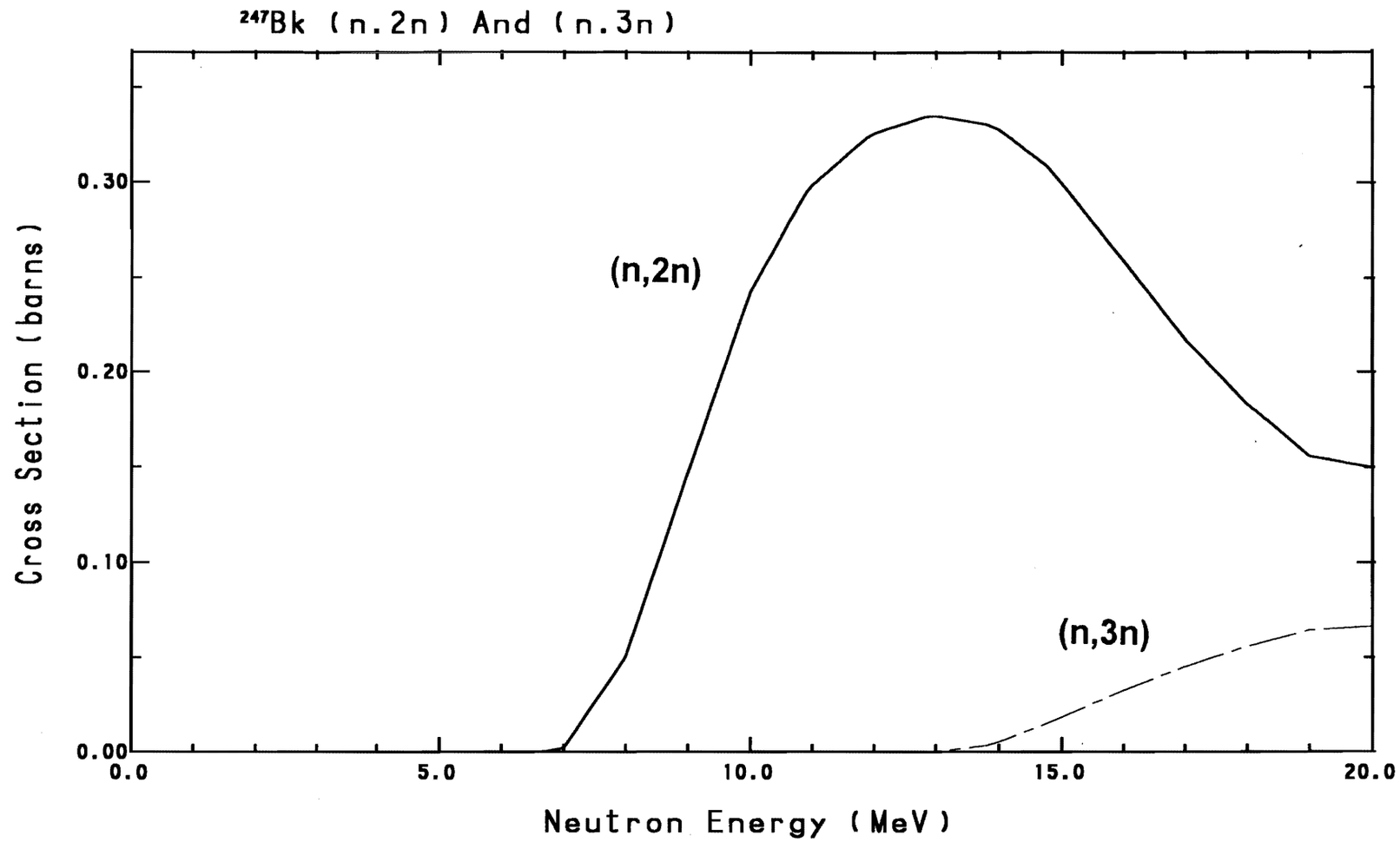

Fig. 3.9 (n,2n) and (n,3n) reaction cross sections of ^{247}Bk

Table 2.1 Level scheme of ^{247}Cm adopted in the previous work[2)]

No.	Energy (keV)	Spin and Parity
Gr.	0.0	9/2 −
1	61.5	11/2 −
2	135.0	13/2 −
3	217.0	15/2 −
4	227.0	5/2 +
5	266.0	7/2 +
6	285.0	7/2 +
7	318.0	9/2 +
8	344.0	9/2 +
9	361.0	11/2 +
10	396.0	11/2 +
11	403.6	1/2 +
12	433.0	3/2 +
13	449.0	5/2 +
14	506.0	1/2 +
15	520.0	3/2 +

Levels above 550 keV were assumed to be overlapping.

Table 2.2 ^{247}Cm resonance parameters below 20 eV

Belanova et al.[6)]			Mughabghab[8)]	Danon et al.[4)]		
E(eV)	Γ(meV)	$2g\Gamma_n$(meV)	Γ_f(meV)	E(eV)	Γ_f(meV)	A_f(b.eV)
1.247	74±4	0.56±0.09	34±7	1.2	34±6	427±24
2.919	70±30	0.1±0.04	30±30			
3.189	130±6	1.0±0.1	62±6	3.1	70±14	444±70
				4.4		107±47
9.55	166±60	0.9±0.33	125±60	9.2	117±83	141±70
18.1	210±170	3.7±1.5	167±170	18.0	166±152	332±46

Table 2.3 ^{247}Cm resonance parameters adopted in the present work

energy (eV)	Γ(eV)	Γ_n(eV)	Γ_γ(eV)	Γ_f(eV)
-3.00000- 1	1.14020- 1	2.00000- 5	3.40000- 2	8.00000- 2
1.24700+ 0	7.45600- 2	5.60000- 4	3.00000- 2	4.40000- 2
2.91900+ 0	7.01000- 2	1.00000- 4	4.00000- 2	3.00000- 2
3.18900+ 0	1.11000- 1	1.00000- 3	4.00000- 2	7.00000- 2
4.40000+ 0	8.63100- 2	2.00000- 3	4.00000- 2	4.43100- 2
9.55000+ 0	1.67730- 1	2.73000- 3	4.00000- 2	1.25000- 1
1.81000+ 1	2.13140- 1	7.14000- 3	4.00000- 2	1.66000- 1
2.13000+ 1	4.44130- 1	1.30000- 4	4.00000- 2	4.04000- 1
2.40300+ 1	1.74044- 1	4.40000- 5	4.00000- 2	1.34000- 1
2.53500+ 1	6.60100- 2	1.00000- 5	4.00000- 2	2.60000- 2
2.61900+ 1	2.60150- 1	1.50000- 4	4.00000- 2	2.20000- 1
2.80400+ 1	9.30580- 2	5.80000- 5	4.00000- 2	5.30000- 2
3.02500+ 1	4.74500- 2	3.45000- 3	4.00000- 2	4.00000- 3
3.06200+ 1	9.21900- 2	1.90000- 4	4.00000- 2	5.20000- 2
3.22300+ 1	6.65100- 2	5.10000- 4	4.00000- 2	2.60000- 2
3.63600+ 1	1.02630- 1	1.63000- 3	4.00000- 2	6.10000- 2
3.77400+ 1	5.95025- 1	2.50000- 5	4.00000- 2	5.55000- 1
3.77600+ 1	5.43300- 2	1.33000- 3	4.00000- 2	1.30000- 2
3.95200+ 1	7.45006- 1	6.00000- 6	4.00000- 2	7.05000- 1
3.99500+ 1	2.07095- 1	9.49999- 5	4.00000- 2	1.67000- 1
4.06100+ 1	8.80320- 2	3.20000- 5	4.00000- 2	4.80000- 2
4.12500+ 1	6.06600- 2	6.60000- 4	4.00000- 2	2.00000- 2
4.17600+ 1	5.86052- 1	5.20000- 5	4.00000- 2	5.46000- 1
4.33900+ 1	4.41900- 2	1.90000- 4	4.00000- 2	4.00000- 3
4.48700+ 1	7.41000- 2	2.10000- 3	4.00000- 2	3.20000- 2
4.52100+ 1	1.00580- 1	5.80000- 4	4.00000- 2	6.00000- 2
4.79200+ 1	2.05170- 1	1.17000- 3	4.00000- 2	1.64000- 1
4.88500+ 1	1.28800- 1	6.80000- 3	4.00000- 2	8.20000- 2
5.00800+ 1	9.73600- 2	2.36000- 3	4.00000- 2	5.50000- 2
5.06900+ 1	9.51800- 2	3.18000- 3	4.00000- 2	5.20000- 2
5.17800+ 1	5.56600- 2	1.66000- 3	4.00000- 2	1.40000- 2
5.21900+ 1	4.52600- 2	1.26000- 3	4.00000- 2	4.00000- 3
5.36300+ 1	3.64450- 1	4.50000- 4	4.00000- 2	3.24000- 1
5.51000+ 1	7.85300- 2	5.30000- 4	4.00000- 2	3.80000- 2
5.61800+ 1	1.09660- 1	6.60000- 4	4.00000- 2	6.89999- 2
5.96600+ 1	1.55570- 1	1.57000- 3	4.00000- 2	1.14000- 1

Total spin J was assumed to be 4.5 for all levels, and the single level Breit-Wigner formula was adopted.

Table 2.4 Thermal cross sections and resonance integrals of ^{247}Cm

Quantity	Reference	data(barns)
σ_{cap}	78Gavrilov[29]	60
	Mughabghab[8]	57±10
	ENDF/B-VI[15]	58.2
	JENDL-3.2[2]	57.2
	Present	55.0
σ_{fiss}	70Halperin[30]	120±12
	72Benjamin[31]	82±5
	76Zhuravlev[32]	80±7
	91Danon[4]	106±53
	Mughabghab	81.9±4.4
	ENDF/B-VI	83.4
	JENDL-3.2	81.8
	Present	103.4
RI_{cap}	78Gavrilov	490
	Mughabghab	530±30
	ENDF/B-VI	492.0
	JENDL-3.2	534.6
	Present	543.9
RI_{fiss}	70Halperin	1060±110
	72Benjamin	778±50
	76Zhuravlev	730±70
	91Danon	890±53
	Mughabghab	760±50
	ENDF/B-VI	750.9
	JENDL-3.2	611.7
	Present	876.2

Table 2.5 Adopted level scheme of ^{247}Cm

No.	Energy (keV)	spin-parity	coupling
GS	0.0	9/2 –	*
1	61.5	11/2 –	*
2	135.0	13/2 +	*
3	217.0	15/2 –	
4	227.0	5/2 +	
5	266.0	7/2 –	
6	285.0	7/2 +	

Level above 309 keV were assumed to be overlapping. Level with * were coupled in the ECIS88 calculation.

Table 3.1 Level scheme of ^{247}Bk

No.	Energy (keV)	spin-parity	coupling
GS	0.0	3/2 −	*
1	29.9	5/2 −	*
2	40.8	7/2 +	
3	71.6	7/2 −	*
4	82.8	9/2 +	
5	125.5	9/2 −	*
6	137.0	11/2 +	
7	196.0	13/2 +	
8	265.0	15/2 +	
9	334.9	5/2 +	
10	378.1	7/2 +	
11	447.8	5/2 −	
12	487.0	1/2 +	
13	489.4	7/2 −	
14	518.0	3/2 +	
15	541.0	9/2 −	
16	587.0	13/2 +	
17	704.0	1/2 −	
18	743.0	5/2 −	
19	815.0	7/2 −	
20	828.0	9/2 −	
21	904.0	9/2 −	

Continuum levels were assumed above 983 keV. Level with * were coupled in the ECIS88 calculation.

Table 3.2 Level density parameters

Isotope	a (1/MeV)	Spin-cutoff parameter	Pairing Energy (MeV)	Temperature (MeV)	C (1/MeV)	Ex (MeV)
^{247}Bk	28.1	30.47	0.39	0.364	2.90	7.97
^{248}Bk	27.8	30.39	0.0	0.326	10.8	1.85

Table 3.3 Thermal cross sections and resonance integral of ^{247}Bk

quantity	value
σ_{total}	288
$\sigma_{elastic}$	12.3
$\sigma_{fission}$	92
$\sigma_{capture}$	184
$RI_{fission}$	453
$RI_{capture}$	896